

# Estimating The Sodium Ion Diffusion Coefficient in Rat Brain

James A. Goodman<sup>1</sup>, G. Larry Bretthorst<sup>2</sup>, Christopher D. Kroenke<sup>2</sup>,  
Joseph J. H. Ackerman<sup>1,2,3</sup>, Jeffrey J. Neil<sup>2,4</sup>

*Departments of Chemistry,<sup>1</sup> Radiology,<sup>2</sup> Internal Medicine,<sup>3</sup> and Neurology – Division of Pediatrics<sup>4</sup>  
Washington University, One Brookings Drive, St. Louis MO 63130*

**Abstract.** Quantifying sodium ion diffusion in the extra- and intracellular compartments will provide mechanistic insight into the as yet unexplained marked decrease in water diffusion resulting from central nervous system injury. As a first step, the apparent diffusion coefficient (ADC) of bulk brain Na<sup>+</sup> has been determined in vivo in rat. A surface coil transmit/receive adiabatic-pulse scheme is used to provide two dimensions of volume localization, thus minimizing echo time. The third dimension is determined by slice selection gradients on the axis perpendicular to the coil plane. Signal decay in the presence of diffusion sensitizing pulsed field gradients was modeled by Bayesian Probability Theory. Preliminary findings indicate a bulk Na<sup>+</sup> ADC of  $(1.16 \pm .07) \times 10^{-3} \text{ mm}^2/\text{s}$ .

## INTRODUCTION

The rate constant governing water incoherent displacement in tissue, the apparent diffusion coefficient (ADC), is observed to decrease drastically following various injuries in brain tissue [1-6]. Clinicians have exploited this phenomenon over the past decade to make magnetic resonance images in which voxel intensity is a function of ADC. This results in images that have a high contrast distinguishing the region of injured or impaired tissue. This has proven to be an important development in diagnostic medicine.

Though this phenomenon is exploited daily in the clinical setting, the underlying biophysical mechanisms are not well understood. Knowledge of the changes of water incoherent displacement motion in the intra and extracellular compartments following injury will provide an important step towards the elucidation of these mechanisms. Unfortunately, there exists no good way to resolve the water MR signal in these two spaces. One strategy for making inferences about the motion of the water in each of these compartments is to employ MR-active chemical species present in the water in either or both spaces that can be compartmentally distinguished.

Sodium is one such species. Sodium is a good choice because the amounts of intracellular and extracellular sodium ion (Na<sup>+</sup>) are within the same order of magnitude and the high extracellular to intracellular concentration gradient is an essential marker of the health of cells. As a first step, the total tissue sodium ADC should be measured. Here we present a method for determining the ADC of total tissue sodium in rat brain.

Sodium ion concentration in the extracellular space, which comprises roughly 20% of the brain tissue, is approximately 140 mM, while sodium ion concentration in the intracellular space is roughly 10 mM. The bulk of the signal, roughly 80% (without diffusion weighting), therefore is from sodium residing in the extracellular space. Without compartmental MR signal resolution, however, it would be incorrect to attribute the resulting ADC completely to the motion of sodium in either space.

NMR diffusion studies in vivo of tissue sodium are rather difficult. First of all, sodium has a low magnetogyric ratio,  $\gamma$ , precessing at only one fourth the frequency of protons in a given magnetic field. As a result (*vide infra*), very strong diffusion encoding magnetic field gradients are needed to attain appropriate diffusion weighting. In addition, sodium ion concentrations are very low, about 40 mM bulk. Thus, to achieve acceptable signal-to-noise ratio, the average of many signal transients is needed. Furthermore,  $^{23}\text{Na}$  is a quadrupolar nucleus, resulting in a very short transverse (observable) magnetization coherence time constant,  $T_2$ , of about 34 ms. (A second  $T_2$  component of about 5 ms has also been observed, but the echo time of our experiment is such that the fast component has decayed away and does not comprise a significant fraction of the signal.) After the experiment begins, the recoverable signal decreases by a factor of  $e$  every 34 ms. These factors require echo time to be minimized, diffusion gradients to be maximized, and the repetition time of the experiment to be short. This results in a high duty cycle for the spectrometer.

We chose rats as the subject for this experiment because multiple injury models, such as stroke, status epilepticus, and others, are well established in these animals. Rats also have the largest brain (and therefore the most signal) that our experimental setup can reasonably support.

Presented here is a technique for measuring sodium ion diffusion in live rat brain. These measurements were performed using a small two-turn ellipsoidal surface radio-frequency (RF) transmit/receive coil (1.4 cm on long axis, 1.0 cm on short axis). These dimensions were chosen so that the region of excitation of the coil would determine two dimensions of the region of interest. A surface coil was chosen because it provides high signal sensitivity. The surface coil sits directly on the rat's skull immediately above the brain. Adiabatic pulses were used for RF excitation to maximize the volume interrogated by the surface coil, and because they provide excellent slice selection for the third dimension of localization. The total sodium ion ADC was found to be  $(1.16 \pm .07) \times 10^{-3} \text{ mm}^2/\text{s}$ .

## MATERIALS AND METHODS

### Animal Preparation

Ten male Sprague Dawley rats, 250 to 350-g, were anesthetized with a dose of a 1.2-ml/100-g 10% urethane solution. A booster dose of 0.6-ml/100 g of the same solution was administered 30 min later. Animals were placed in an MR compliant stereotaxic head frame and ventilated with 100%  $\text{O}_2$ . Body temperature was maintained by circulating warm water through a flat network of Tygon<sup>®</sup> (plastic) tubes

on which the animal rests. Body core temperature was monitored rectally with a fiber optic temperature probe (Fiso, Sainte-Foy), heart rate and oxygen saturation were monitored with a pulseoximeter (Nonin, Minneapolis).

## Magnetic Resonance Experiments

Imaging and spectroscopy experiments were performed using an Oxford Instruments, 33 cm diameter clear bore, 4.7 tesla magnet equipped with 10cm-inner diameter actively shielded gradient coil system capable of producing linear magnetic field gradients of up to 60 G/cm. A Varian NMR Systems (Palo Alto, CA) INOVA console controls the magnet and gradient systems. Experiments were performed with a 4 cm single turn surface coil for  $^1\text{H}$  measurements, and a 1 x 1.4 cm two-turn ellipsoidal surface coil for  $^{23}\text{Na}$  experiments. The proton coil is placed along the side of the rat's head, centered on the brain (Fig. 1). The sodium coil is oriented orthogonally to the proton coil (to minimize RF cross talk), directly above the brain of the animal. LASER (*localization by adiabatic selective refocusing*) pulse sequences were used for all spectroscopy experiments to mitigate the effects of the inhomogeneous interrogating RF fields created by the surface coils [7].

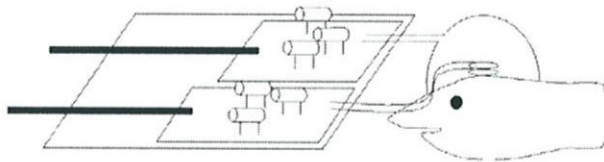


**FIGURE 1.** Diagram of the MR RF transmit/receive apparatus. The setup includes two separate RF coils, a 4 cm single turn proton coil and a 1.4 cm (long axis) x 1.0 cm (short axis) two-turn ellipsoidal sodium coil.

Brain tissue  $^1\text{H}_2\text{O}$  or  $^{23}\text{Na}^+$  diffusion is measured with the LASER sequence in the following manner (Fig. 2). After the magnetization is placed in the transverse (observation) plane with  $90^\circ$  RF pulse, the nuclear moment (spin) of each  $^1\text{H}_2\text{O}$  or  $^{23}\text{Na}^+$  is “wound up” to a unique, spatial-position-dependant phase using a pulsed magnetic field gradient. After a given amount of time, a  $180^\circ$  RF refocusing causes a phase inversion, and a second pulsed magnetic field gradient is used to “unwind” the phases. If diffusion has taken place, the phases will either “unwind” too far or not far enough, and the net magnetization vector, and therefore echo intensity, will be attenuated. If the strength of the diffusion sensing gradients is increased, the experiment will be more sensitive to the diffusion of spins. This allows a series of spectra to be taken whose echo signal amplitudes decay exponentially as a function of the diffusion weighting term  $b$  (*vide infra*) with a rate constant equal to the ADC.

Notice that only one dimension of localization, the depth, results from the pulse sequence. The other two dimensions are provided by the size of the coil itself and its RF transmission/reception range. The resulting volume element has the shape of a flattened ellipsoidal cylinder, centered in the brain.

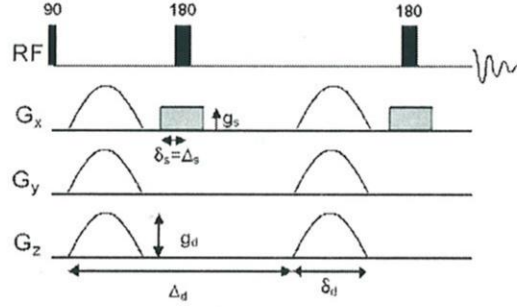


**FIGURE 2.** A LASER experiment with slice selection on the  $G_x$  axis alone, where  $G_x$  is the direction perpendicular to the plane of the sodium coil.  $g_d$  is the strength of the diffusion encoding gradients,  $\Delta_d$  is the time separating the diffusion gradients, and  $\delta_d$  is the length of the diffusion encoding gradients. The second  $180^\circ$  refocusing RF pulse is required to reverse the non-linear phase induced by the first  $180^\circ$  refocusing RF pulse.

## Data Analysis

All data was analyzed with the Bayesian Analysis Package developed in our laboratory and interfaced to Varian's operating/analysis software package "VNMR". The raw time domain data (the spin echo) contain a single exponentially decaying sinusoid, the  $^{23}\text{Na}^+$  or  $^1\text{H}_2\text{O}$  MR signal. Bayesian probability theory was used to estimate the amplitude, phase, frequency and decay rate constant of this sinusoid. For our purposes, the amplitude is the parameter of interest. After this initial estimation stage, a second Bayesian calculation was performed. The estimated amplitudes of the sinusoids are a function of diffusion weighting,  $b$ , as described by Stejskal-Tanner [8], and modeled as:

$$S(b) = A e^{-b \cdot \text{ADC}} + \text{noise} \quad (1)$$

where  $b$  is given by [9]

$$b = \gamma^2 \int_{t=0}^T \left( \int_{t=0}^t G(t') dt' \right)^2 dt. \quad (2)$$

Analytically, for this experiment,

$$b = \gamma^2 \left[ \frac{4}{\pi} g_d g_s \delta_d \delta_s \Delta_s + 2 g_s^2 \delta_s^2 \left( \Delta_s - \frac{\delta_s}{3} \right) + \frac{12}{\pi^2} g_d^2 \delta_d^2 \left( \Delta_d - \frac{\delta_d}{4} \right) \right], \quad (3)$$

where  $g$ 's and  $\delta$ 's represent gradient strengths and timings, respectively, as shown in Fig. 2. The parameters in this exponential model, the amplitude,  $A$ , and the ADC were then estimated using Bayesian probability theory. This second Bayesian calculation was implemented using Markov chain Monte Carlo to draw samples from the joint posterior probability for the amplitude and ADC. Finally Monte Carlo integration was used to approximate the posterior probability for the ADC and the amplitude. We have displayed an example of these two probability density functions in Fig. 3. The widths of these probability density functions are a natural measure of the uncertainty in the estimated parameter values.

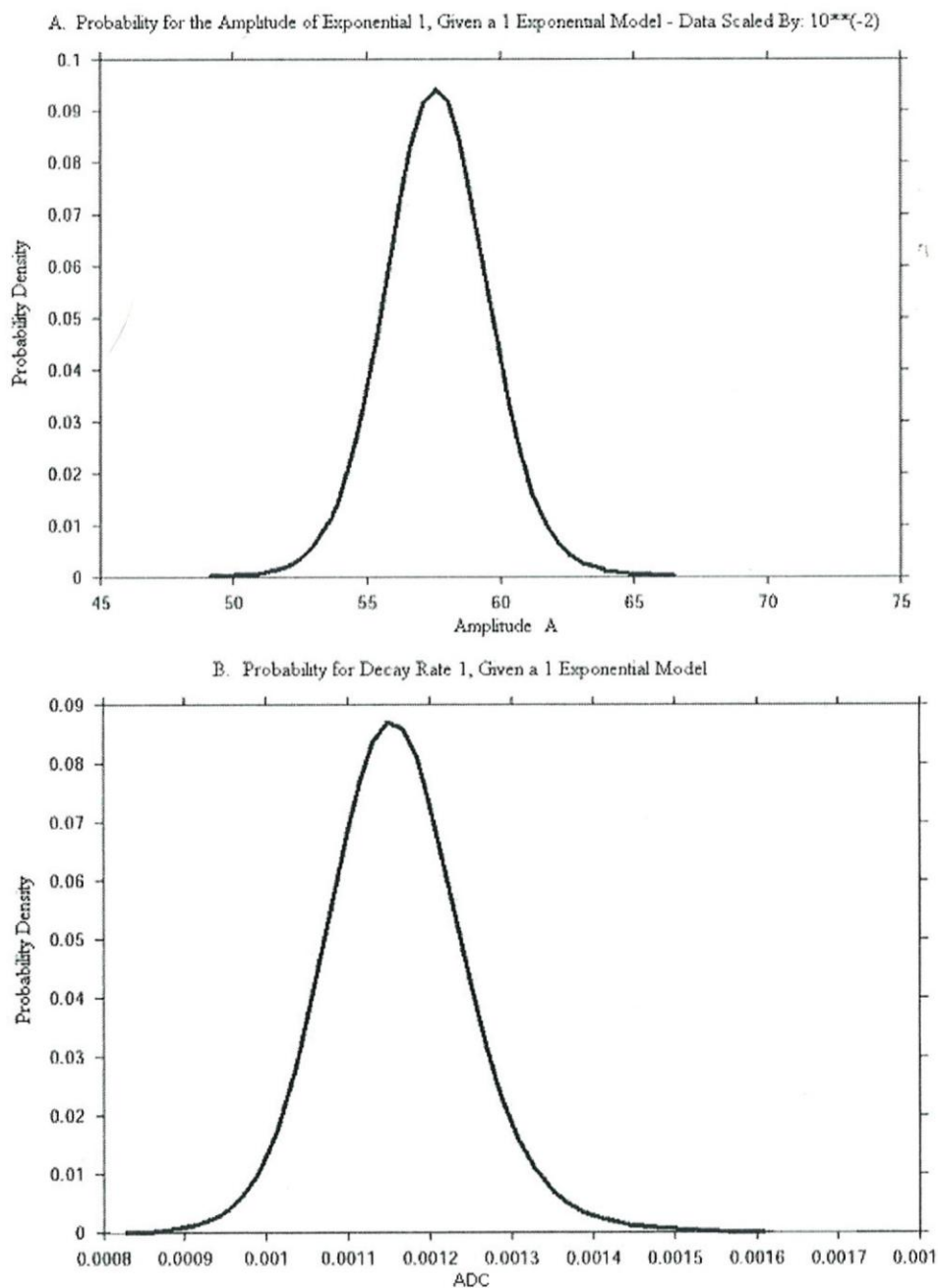


**FIGURE 3.** Panel A is the posterior probability for the amplitude of the exponential function, and panel B is the posterior probability for the exponential decay rate constant, the ADC. The estimated uncertainty for the ADC of sodium ion in this measurement is given by the standard deviation of the posterior probability density function,  $\pm 0.00009 \text{ mm}^2/\text{s}$  in this case.

## RESULTS

Bulk  $^{23}\text{Na}^+$  ADC in this roughly  $0.6\text{-cm}^3$  volume in ten rats was found to be  $1.16 \times 10^{-3} \text{ mm}^2/\text{s}$  with an inter-animal standard deviation of  $0.07 \times 10^{-3} \text{ mm}^2/\text{s}$ . In a similar voxel the water ADC was found to be  $0.83 \times 10^{-3} \text{ mm}^2/\text{s}$  with an inter-animal standard deviation of  $\pm 0.02 \times 10^{-3} \text{ mm}^2/\text{s}$ .

## DISCUSSION

Assuming the intracellular and extracellular  $^{23}\text{Na}^+$  T2s are similar, approximately 80% of the observed signal in these experiments is from  $\text{Na}^+$  in the extracellular space.  $\text{Na}^+$  exhibits rapid displacement motion relative to other non-water tissue species that have been examined [10-12]. As a comparison, ADC values in brain and values of free, unrestricted diffusion in aqueous solutions at  $37^\circ\text{C}$  are shown in table 1 for  $\text{Na}^+$  [13], as well as for  $\text{Cs}^+$  [11] and  $\text{H}_2\text{O}$ , which are approximately 90% and 80% intracellular, respectively. Although diffusion values for all three chemical species are reduced relative to  $D^{\text{free}}$ , the degree of reduction suggests that the intracellular partition is significantly more restrictive to diffusion than is the extracellular space.

TABLE 1.

| species              | $D^{\text{free}}$ | ADC  | % reduced | compartment |
|----------------------|-------------------|------|-----------|-------------|
| $\text{Na}^+$        | 1.9               | 1.16 | 39        | ~80% extra  |
| $\text{Cs}^+$        | 2.7               | 0.91 | 66        | ~90% intra  |
| $\text{H}_2\text{O}$ | 2.9               | 0.83 | 71        | ~90% intra  |

TABLE 1. Comparison of bulk rat brain tissue ADCs and free unrestricted diffusion coefficients,  $D^{\text{free}}$ , for  $\text{Na}^+$ ,  $\text{Cs}^+$ , and  $\text{H}_2\text{O}$ .  $D^{\text{free}}$  and ADC are given in units of  $10^{-3} \text{ mm}^2/\text{s}$ .

An alternative interpretation is that our measurement of the  $\text{Na}^+$  diffusion coefficient in rat brain is somewhat high because a portion of the region of interest includes sodium in cerebral ventricles and/or venous sinuses, which would act as a reservoir of unrestricted diffusion.

## ADKNOWLEDMENTS

This research was funded by NIH grants NS35912 and R24-CA83060, and Department of Education grant P200A00217.

## REFERENCES

1. Moseley, M. E., et. al., *Magn. Reson. Med.* **14**, 330-346 (1990).
2. Zhong, J., et. al., *Magn. Reson. Med.* **33**, 253-256 (1995).
3. Verhuel, H. B., et. al., *Brain Res.* **618**, 203-212 (1993).
4. Ford, J. C., et. al., *Magn. Res. Med.* **31**, 488-494 (1994).

5. Hasegawa Y., et. al., *Stroke* **27**, 1648-1655 (1996).
6. Takano K., et. al., *Ann. Neuro.l* **39**, 308-318 (1996).
7. Garwood M., and DelaBarre, L., *J. Magn. Reson.* **153**, 155-170 (2001).
8. Stejskal, E. O., and Tanner, J. E., *J. Chem. Phys.* **42**, 288-292 (1965).
9. Karlicek, R. F., and Lowe, I. J., *J. Magn. Reson.* **37**, 75-91 (1980).
10. Duong, T. Q., et. al., *Magn. Reson. Med.* **40**, 1-13 (1998).
11. Neil, J. J., et. al., *Magn. Reson. Med.* **35**, 329-335 (1996).
12. Sehny, J. V., et. al., *Magn. Reson. Med.* **48**, 42-51 (2002).
13. Lobo, V. M. M., *Pure & Appl. Chem.* **65**, 2613-2640 (1993).